JACS
JOURNAL OF THE AMERICAN CHEMICAL SOCIETY
pubs.acs.org/JACS
Article

Tunable Adhesion from Stoichiometry-Controlled and Sequence-Defined Supramolecular Polymers Emerges Hierarchically from Cyanostar-Stabilized Anion−Anion Linkages

Wei Zhao, Joshua Tropp, Bo Qiao, Maren Pink, Jason D. Azoulay, and Amar H. Flood*

Cite This: https://dx.doi.org/10.1021/jacs.9b12645
Read Online

ABSTRACT: Sequence-controlled supramolecular polymers offer new design paradigms for generating stimuli-responsive macromolecules with enhanced functionalities. The dynamic character of supramolecular links present challenges to sequence definition in extended supramolecular macromolecules, and design principles remain nascent. Here, we demonstrate the first example of using stoichiometry-control to specify the monomer sequence in a linear supramolecular polymer by synthesizing both a homopolymer and an alternating copolymer from the same glycol-substituted cyanostar macrocycle and phenylene-linked diphosphate monomers. A 2:1 stoichiometry between macrocycle and diphosphate produces a supramolecular homopolymer of general formula $(\mathbf{A})_n$ comprised of repeating units of cyanostar-stabilized phosphate−phosphate dimers. Using a 1:1 stoichiometry, an alternating $(\mathbf{AB})_n$ structure is produced with half the phosphate dimers now stabilized by the additional counter cations that emerge hierarchically after forming the stronger cyanostar-stabilized phosphate dimers. These new polymer materials and binding motifs are sufficient to bear normal and shear stress to promote significant and tunable adhesive properties. The homopolymer $(\mathbf{A})_n$, consisting of cyanostar-stabilized *anti*-electrostatic linkages, shows adhesion strength comparable to commercial superglue formulations based on polycyanoacrylate but is thermally reversible. Unexpectedly, and despite including traditional ionic linkages, the alternating copolymer $(\mathbf{AB})_n$ shows weaker adhesion strength more similar to commercial white glue based on poly(vinyl acetate). Thus, the adhesion properties can be tuned over a wide range by simply controlling the stoichiometric ratio of monomers. This study offers new insight into supramolecular polymers composed of custom-designed anion and receptor monomers and demonstrates the utility of emerging functional materials based on anion−anion linkages.

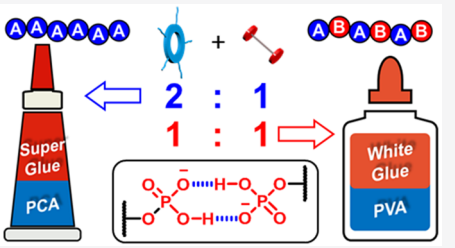

INTRODUCTION

Emerging technologies derived from responsive supramolecular polymers[1,2] benefit from the creation of versatile macromolecules with synthetically engineered functionalities.[3,4] Interest in supramolecular polymers[5−7] continues unabated owing to the unique properties conferred by their noncovalent connectivities and dynamic structures,[8,9] as well as their potential for applications in biomedicine,[10,11] optoelectronics,[12,13] and adaptive materials.[14,15] These applications benefit from chemically unique and reconfigurable macromolecular linkages combined with well-defined sequences of monomer units.[6,16] Pioneering efforts to control the sequences of supramolecular polymers have relied on monomers encoded with orthogonal supramolecular linkages, e.g., hydrogen bonding,[17] metal−ligand coordination,[18] and host−guest recognition.[19] These include heterotopic monomers bearing end-groups with orthogonal linkage chemistries,[20−29] and use of two different homotopic monomers with complementary binding partners at either end.[30−33] The orthogonal monomers enable self-sorting to define supramolecular polymer sequences.[28,34] However, use of a single homotopic monomer to achieve sequence control is unknown. This outcome appears to be a contradiction given that the identical end-groups do not offer preprogrammed orthogonality. Here we report the discovery of a single homotopic dianion monomer (Figure 1a) that combines with a macrocycle (Figure 1b) where orthogonal recognition chemistries emerge hierarchically (Figure 1c) to enable control over monomer sequence in supramolecular homopolymers (Figure 1d) and alternating[35,36] copolymers (Figure 1e) simply by changing reaction stoichiometry.

Previous studies have demonstrated that variation in the reaction stoichiometry of the monomers can control various features of supramolecular polymers. These include the topology by toggling between linear and cross-linked states,[37−39] and net chirality.[40−42] Use of the stoichiometry to control the sequences in linear supramolecular polymers, however, remains nascent. The role of stoichiometry is well established in small molecule chemistry. Different host−guest complexes can be made by altering stoichiometry,[37,38] but this

Received: November 23, 2019
Published: January 14, 2020

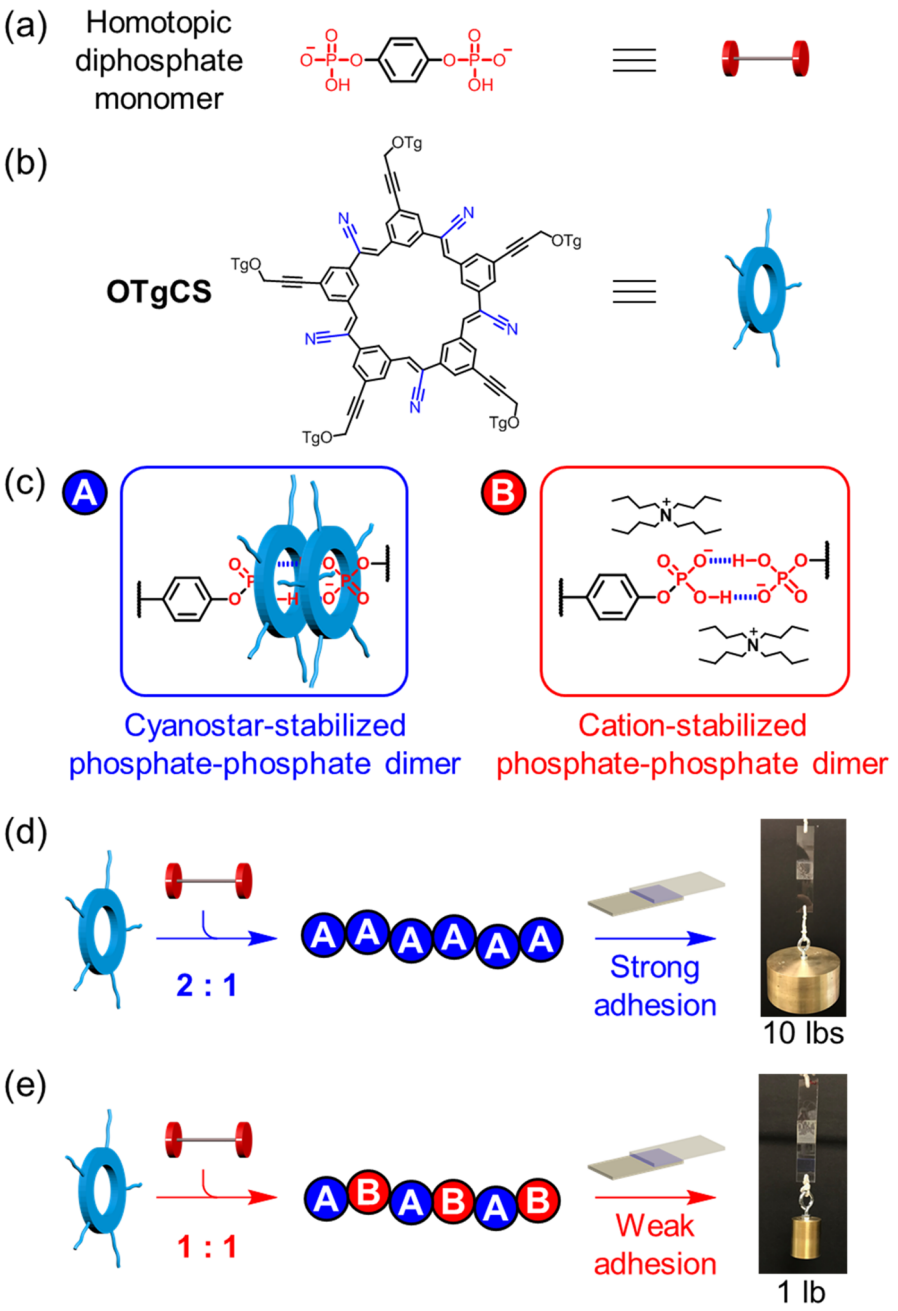

Figure 1. Structures of (a) the homotopic diphosphate with a rigid phenylene linker, (b) the new cyanostar macrocycle, **OTgCS**, and linkage chemistries of (c) cyanostar-stabilized phosphate−phosphate dimer (**A**) and cation-stabilized phosphate−phosphate dimer (**B**). Representation of stoichiometry-controlled supramolecular polymers: (d) homopolymer $(\mathbf{A})_n$ shows strong adhesion, and (e) the alternating copolymer $(\mathbf{AB})_n$ shows weak adhesion.

functionality has yet to be leveraged for controlling sequences in supramolecular polymers. There are, in general, very few reported examples of using stoichiometry control. Among them, the closest involves addition of 3 mol % of Eu^{2+} to a linear zinc-coordinated supramolecular polymer to drive cross-linking.[39] In pioneering work from Sessler,[43] stoichiometry was evident when using cationic macrocycles, called "Texas-sized" boxes, combined with terephthalate monoanions where changing the monomer ratio from 3:2 to 1:1 drove a transition from a small-molecule complex to a supramolecular polymer. In this case, however, the sequence of the supramolecular polymer was not tunable. These examples highlight the underdeveloped nature of this approach to control the sequence of supramolecular polymers. To the best of our knowledge, stoichiometry has not been used to control the sequence of monomers to form well-defined supramolecular homopolymers and alternating copolymers.

To construct supramolecular polymers, reliable noncovalent interactions with high affinity and fidelity are essential.[3] To date, many well-defined recognition chemistries have been developed and exploited to synthesize supramolecular polymers. The majority of examples are based upon metal-coordination,[44] hydrogen bonding,[45,46] $\pi-\pi$ interactions,[47,48] and host−guest interactions.[49,50] Studies involving anion coordination as the driving force for supramolecular polymerization, however, account for less than 1% of the >10,000 re-

https://dx.doi.org/10.1021/jacs.9b12645
J. Am. Chem. Soc. XXXX, XXX, XXX−XXX

Scheme 1. Synthetic Scheme for Preparation of Penta-Substituted Cyanostar Macrocycle, OTgCS

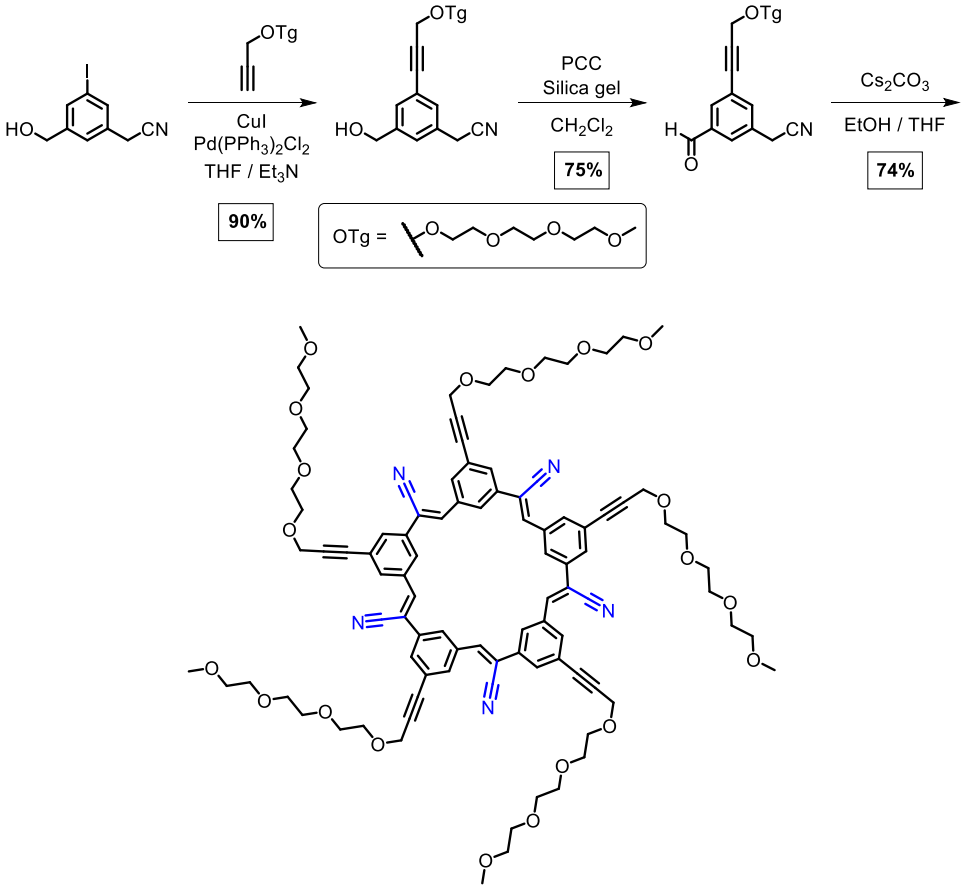

ports. We[51,52] and others[21,43,53−59] have recently been working toward filling this gap by exploring the novel noncovalent chemical connectivities promoted by anion receptors and anionic monomers. We leveraged the high-fidelity dimerization of phosphonate hydroxyanions inside cyanostar macrocycles as the driving force necessary for the formation of well-defined supramolecular polymers.[52] The cyanostar-stabilized anion−anion dimer constitutes a 2:2 recognition motif. Therein, two (2) hydroxyanions dimerize through *anti*-electrostatic hydrogen bonding[60−66] inside a π-stacked pair (2) of cyanostar macrocycles. Although the elementary recognition has been verified with bisulfate dimers $(HSO_4\cdots HSO_4)^{2-}$,[67−69] dimers of dihydrogen phosphate $(H_2PO_4\cdots H_2PO_4)^{2-}$,[70,71] and in polymerization of phosphonate monomers $(RHPO_3\cdots RHPO_3)^{2-}$,[52] the investigation and development of this anion recognition chemistry into a useful tool for supramolecular polymer-based materials is far from developed. In our previous study of supramolecular polymerization driven by phosphonate dimerization,[52] precipitation of a relatively low molecular weight product limited subsequent studies to better understand and elucidate the design principles governing anion−anion driven supramolecular polymerizations.

In this present work, we leverage the inherent modularity of anion−anion dimerization to create new supramolecular connectivities, and present the first example where stoichiometry generates well-defined supramolecular polymers with controlled sequences. We designed a cyanostar that is penta-substituted with triethylene glycol chains (**OTgCS**, Figure 1b) to overcome the solubility issues associated with the parent cyanostar (**tBuCS**).[72] We combined these macrocycles with a rigid diphosphate monomer bearing two identical phosphate end-groups connected by a single phenyl ring (Figure 1a). We discovered that the stoichiometric ratio between building blocks controls the sequence of supramolecular linkages present in the resulting polymers (Figure 1c). A 2:1 stoichiometry between macrocycle and diphosphate monomer produces a supramolecular homopolymer, $(\mathbf{A})_n$, with repeat units of identical 2:2 anion-receptor recognition units. When combined in a 1:1 stoichiometry, however, two types of supramolecular linkages arranged in an alternating sequence define an alternating copolymer $(\mathbf{AB})_n$. These links include the preprogrammed *anti*-electrostatic 2:2 anion-receptor recognition of (**A**), and an unexpected link, (**B**), based on a phosphate−phosphate dianion dimer stabilized by ion pairing with the tetrabutylammonium counter cations (Figure 1c). We demonstrate the use of these materials as a new class of anion-coordination driven supramolecular polymer adhesives.[73−80] The homopolymer comprised of cyanostar-stabilized phosphate dimers is sufficiently cohesive to glue hydrophilic glass slides together to support relatively heavy weights (10 lbs) while the alternating copolymer, with half the links composed of cation-stabilized anion−anion dimers, shows much weaker adhesion. We see **OTgCS** macrocycles are also capable of supporting strong adhesion on account of π-stack mediated self-association of macrocycles. Putative hydrogen bonding from the glass surface to the **OTgCS** macrocycle's glycol chains operates in concert with the supramolecular polymerization to promote the adhesion. The adhesion properties correlate to the sequences of the supramolecular polymers allowing for the development of structure−property relation-

https://dx.doi.org/10.1021/jacs.9b12645
J. Am. Chem. Soc. XXXX, XXX, XXX−XXX

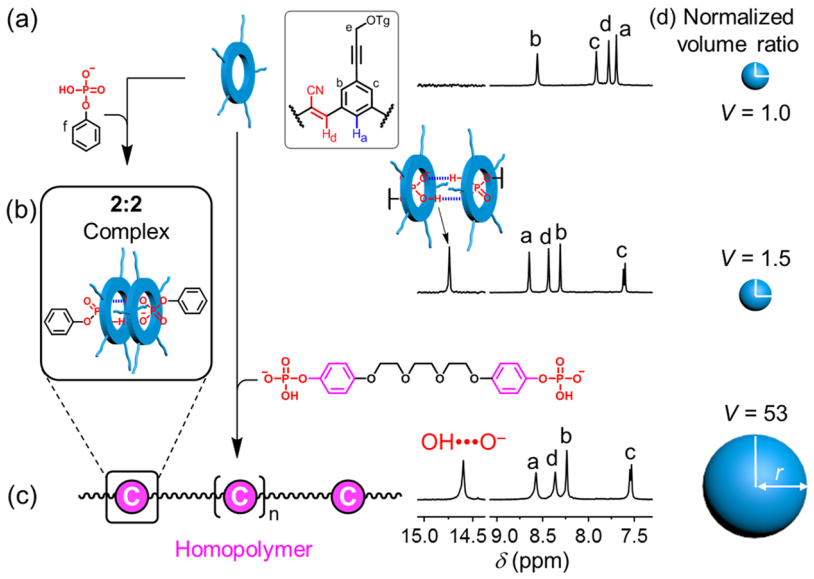

Figure 2. Representations and stacked ^{1}H NMR spectra of (a) **OTgCS**, (b) the small-molecule 2:2 complex, and (c) the supramolecular polymer $(\mathbf{C})_n$. (d) Normalized size comparisons were determined from diffusion coefficients based on the Stokes−Einstein equation ($D = \frac{k_B T}{6\pi\eta r}$) and the spherical model ($V = \frac{4}{3}r^3$), V is proportional to $\frac{1}{D^3}$ ([**OTgCS**] = 10 mM, [phenyl monophosphate] = 10 mM, [triethylene glycol bis(phenyl-*p*-phosphate)] = 5 mM, CD_2Cl_2, 298 K, 600 MHz).

ships for anion−anion driven supramolecular polymers and design principles for anion-based materials.

RESULTS AND DISCUSSION

Molecular Design. The **OTgCS** cyanostar was synthesized with five triethylene glycol chains (Scheme 1) to enhance solubility for studying polymerization at high concentrations. Ethylene glycol chains are also commonly incorporated into synthetic adhesives to enable strong hydrogen bonding interactions with hydrophilic surfaces. The length of the glycol chain was designed to provide sufficient solubility and adhesion properties without adversely impacting purification using chromatography. The modified **OTgCS** macrocycle was made in high yield following the same procedure as the parent cyanostar, **tBuCS**.[72] The new cyanostar achieved the desired goals with enhanced solubility in common organic solvents such as dichloromethane, acetonitrile, and methanol and demonstrated a similar anion-binding profile as the parent **tBuCS** macrocycle toward both PF_6^- (Figure S11) and phenyl monophosphate (Figure S12).

Two types of difunctional monomers were originally designed to help study the dependence of monomer structure on polymerization. A long flexible monomer, triethylene glycol bis(phenyl-*p*-phosphate), was used for initial polymerization studies. Its flexibility mimics the dodecylene diphosphonate we used previously to demonstrate polymerization with **tBuCS**.[52] This flexible monomer was expected and found to behave similarly, providing confirmation that the hydroxyanion dimerization could be used as preprogrammed supramolecular links with both diphosphates as well as the original diphosphonates. To conduct structure−property studies, we also selected a short and rigid phenylene diphosphate monomer. We initially hypothesized that it may limit supramolecular polymerization on account of steric interactions and decreased polymer solubility. We did not anticipate the structural difference between the two monomers would manifest in the stoichiometric control of the supramolecular polymer sequence reported herein.

2:2. Model Complex between Phenyl Monophosphate and Cyanostar. We used the 2:2 complexation between phenyl monophosphate and the **OTgCS** macrocycle as a small-molecule model of the linkage chemistry expressed in the supramolecular polymers. The 2:2 complex forms with high fidelity as seen in a titration monitored by ^{1}H NMR spectroscopy (Figure S12). A number of features are similar to the complexation of phenyl monophosphate with the parent cyanostar **tBuCS**.[70] The uncomplexed **OTgCS** macrocycle shows similar aromatic peak positions as **tBuCS** (Figure 2a). Upon addition of 1.0 equiv of phenyl monophosphate, we see a characteristic signature of the 2:2 linkage (Figure 2b). The far downfield shifted peak at 14.7 ppm is assigned to the phosphate's OH peak, and its position is diagnostic of the formation of a self-complementary hydrogen bond between the two phosphates and, thus, confirmation of phosphate dimerization.[67] The anion dimers are formed inside the cavity of π-stacked macrocycles as established in previous reports.[70] Confirmation of the macrocycle dimers stems from the two H_c peaks (7.6 ppm, Figure 2b) assigned to diastereomers. Single cyanostars are a racemic mixture of rapidly interconverting *M* and *P* enantiomers that are known to form into meso (*MP*) and chiral (*MM* and *PP*) combinations upon 2:2 complexation.[72,81] Resolution of the two diasteromeric complexes (meso and chiral) indicates exchange between them is slow on the NMR time scale. The formation of the 2:2 complex is also supported by diffusion NMR. The diffusion values obtained from the cyanostar (H_c) and the phenylene monophosphate (H_f) are identical and generate a volume that is 1.5 times larger than the free macrocycle (Figure 2d).

Supramolecular Homopolymer Using the Flexible Diphosphate Monomer. To verify that the diphosphate monomers can be combined with the **OTgCS** macrocycle to form supramolecular polymers, we used the flexible triethylene glycol bis(phenyl-*p*-phosphate) to synthesize homopolymers

https://dx.doi.org/10.1021/jacs.9b12645
J. Am. Chem. Soc. XXXX, XXX, XXX−XXX

$(C)_n$. These two components were mixed at a 2:1 ratio to match the equivalence point for the formation of the 2:2 macrocycle/phosphate linkage chemistry (Figure 2c). Using the 2:2 complex as a model, we see the same diagnostic OH peaks at 14.6 ppm indicating the formation of the encapsulated phosphate−phosphate dimers (Figure 2c). We also see characteristic peak shifts (8.1−8.6 ppm) and the diastereomeric splitting in proton H_c all consistent with a complexed cyanostar dimer. Together, these observations confirm the formation of the 2:2 linkage chemistry. Indicative of polymerization, the diffusion NMR shows a dramatic 35-fold increase in size relative to the model complex (Figure 2d). This change is consistent with the 64-fold difference seen previously with the supramolecular polymer made from **tBuCS** and dodecylene diphosphonate.[52] These results confirm that supramolecular polymerization can be achieved using flexible monomers with a reliable preprogrammed linkage chemistry composed of cyanostar-stabilized phosphate dimers.

Alternating Supramolecular Copolymer in the Solid State Using Crystalline Cyanostars. We were surprised to observe a different supramolecular polymer sequence in the solid state when using the rigid phenylene diphosphate monomer in place of the flexible one. In this case, the more crystalline **tBuCS** cyanostar was used in place of **OTgCS** to determine the crystal structure of the supramolecular polymer. The crystal structure shows two different types of phosphate−phosphate dimers (Figure 3). As expected from all prior studies, we see the 2:2 linkage chemistry highlighted as (**A**). Therein, the *anti*-electrostatic phosphate−phosphate dimer is encapsulated by two π-stacked macrocycles. The anion dimers are stabilized by a combination of self-complementary hydrogen bonding and the CH hydrogen bonding from the cyanostars.[67,70] The second type of linkage, highlighted as (**B**), was unanticipated. This new link is also composed of phosphate−phosphate dimers, but are not complexed by cyanostars. These dimers engage in one direct phosphate−phosphate hydrogen bond and one methanol-bridged hydrogen bond between the two phosphates. As with all hydroxyanion dimers, theoretical studies[60−64] show that these *anti*-electrostatic hydrogen bonds are insufficient alone to fully stabilize the dimers. Rather, we infer electrostatic stabilization from the close proximity of the four tetrabutylammonium cations (TBA^+). These cations surround and enshroud the doubly charged phosphate dimers $[(RHPO_4)\cdots(RHPO_4)]^{2-}$ (Figure 3). From the six examples[52,67,68,70,71,82] previously studied using cyanostar stabilization, only one[71] shows this type of superstructure when dihydrogen phosphate ($H_2PO_4^-$) was mixed with cyanostar and cocrystallized with an additional equivalent of TBA^+ salt. These types of close anion−cation contacts are more common to salts of hydroxyanion crystallized in the absence of any receptors.[83,84] In those prior cases, such as in the dimer of bisulfate $[(HSO_4)\cdots(HSO_4)]^{2-}$ stabilized by tetrabutylammonium,[67] there are an equal number of charged counter cations. In the case here, there are four cations proximal to the two exposed anions.

The alternating configuration of phosphate dimers, A−B−A−B etc., is believed to come as a result of the hierarchical assembly in the densely packed solid state. Hierarchical bond formation dictates that the strongest bonds are formed first followed by the less stable ones. We hypothesized that the dimers stabilized by the charge-neutral cyanostar macrocycles are stronger than ones stabilized electrostatically by the

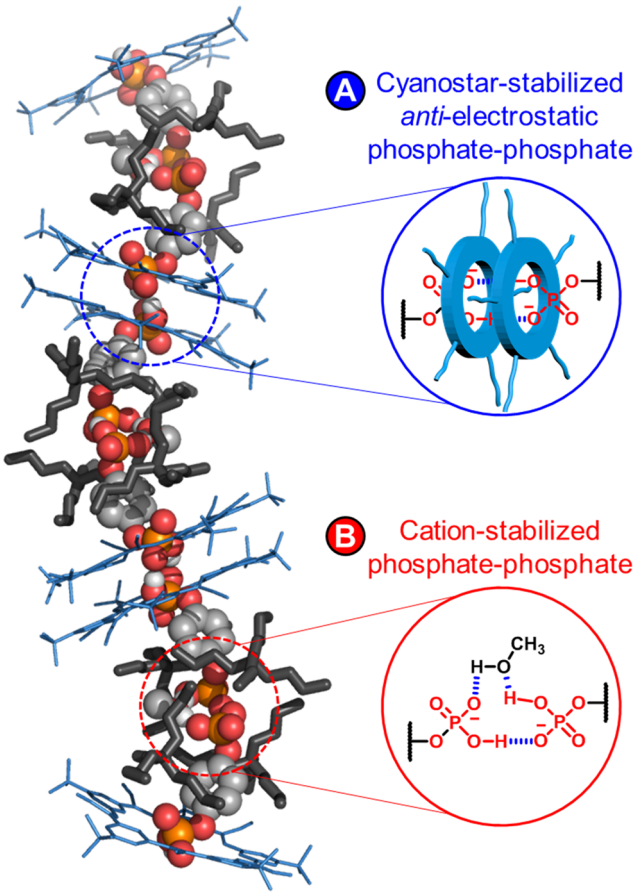

Figure 3. Crystal packing structure of the supramolecular copolymer $(AB)_n$ composed of **tBuCS** macrocycles (blue tube) and phenylene diphosphate (space-filling) as TBA^+ salts (black stick). TBA^+ counter cations encircle the uncomplexed phosphate dimers in (**B**) links. Structures of the phosphate−phosphate dimer encapsulated inside paired macrocycles (**A**) and the methanol-bridged phosphate−phosphate dimer (**B**) are highlighted.

counter cations. Consistent with this idea, cyanostar-stabilized anion−anion dimers are stable in a range of conditions without relying on ion pairing.[68] When the receptors are not present, anion dimers demand high concentrations to form, offer more ambiguous signatures, and presumably rely on ion pairing for enhanced stabilization.[71] Therefore, formation of cyanostar-stabilized dimer (**A**) liberates two counter cations for use elsewhere in the assembly. All together, the uncomplexed phosphate dimers (**B**) have four stabilizing cations. The four cations emerge from the hierarchical assembly, which is believed to be a key step to form the alternating sequence in the copolymer.

The distance dependence of electrostatic interactions suggests that the length of the phenylene linker is also important for copolymer formation. The linker is short enough to help bring multiple negative charges close to each other to enhance the electrostatic stabilization.[85,86] Consistent with this idea, use of long dodecylene diphosphonate[52] or the long and flexible diphosphate monomers fails to produce the alternating copolymer in solution or the solid state. A competing hypothesis is that the alternating sequence emerges as a result of steric repulsion between macrocycles. However, the phenylene linker is also long enough to accommodate all the macrocycles. The goldilocks effect appears to be in play. The

https://dx.doi.org/10.1021/jacs.9b12645
J. Am. Chem. Soc. XXXX, XXX, XXX−XXX

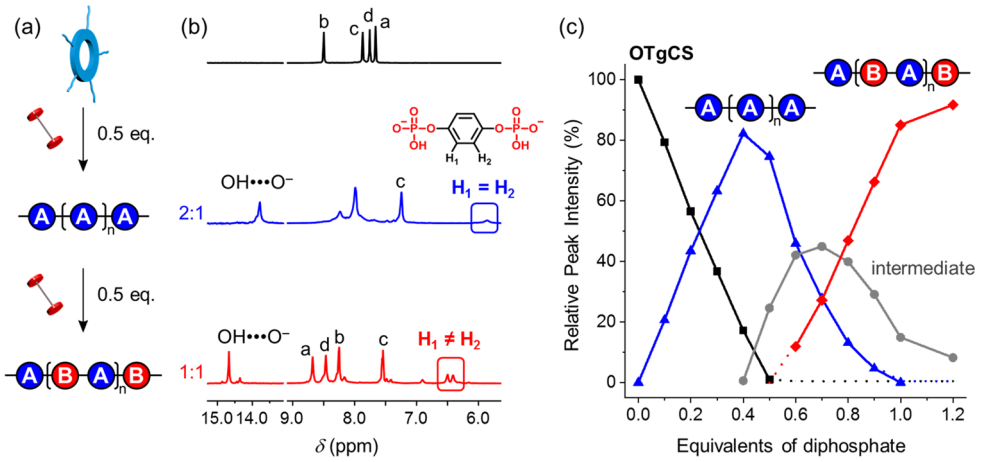

Figure 4. (a) Representation for the stoichiometry-controlled supramolecular polymerization. (b) Stacked ^{1}H NMR spectra of **OTgCS**, supramolecular homopolymer $(\mathbf{A})_n$, and alternating copolymer $(\mathbf{AB})_n$ ([**OTgCS**] = 5 mM, CD_2Cl_2, 298 K, 600 MHz). (c) Relative peak intensity changes of the free macrocycle, the supramolecular homopolymer $(\mathbf{A})_n$, the alternating supramolecular copolymer $(\mathbf{AB})_n$, and intermediate species as a function of increasing amount of phenylene diphosphate.

phenylene is not too big nor too small but just right for producing the copolymer. We also attempted to form the homopolymer in the solid state by increasing the relative amount of **tBuCS** macrocycles during crystallization but without success. This specific finding suggests that the ionic interactions may be larger than expected. Thus, it was not clear from the crystal structure if the hierarchical assembly of the rigid phenylene diphosphate into an alternating supramolecular copolymer $(\mathbf{AB})_n$ is driven by the cyanostars or the cations.

Stoichiometry-Controlled Supramolecular Copolymers in Solution. Inspired by the two types of phosphate−phosphate linkages seen in the crystal structure, we hypothesized that the alternating copolymer and homopolymer configurations could form in solution by stoichiometry control (Figure 4a). We expected to produce the supramolecular homopolymer $(\mathbf{A})_n$ composed solely of preprogrammed cyanostar-stabilized phosphate dimers by using a 2:1 stoichiometric ratio between macrocycle and phenylene diphosphate. Adjusting the stoichiometry to a 1:1 ratio would then be expected to form the alternating supramolecular copolymer $(\mathbf{AB})_n$ seen in the solid state.

As anticipated, we were able to use stoichiometry to prepare both types of supramolecular polymers: the $(\mathbf{A})_n$ homopolymer and $(\mathbf{AB})_n$ copolymer. Significantly, the **OTgCS** macrocycle provided the increased solubility needed to explore stoichiometry control. Elevated concentrations were not possible using **tBuCS** on account of significant precipitation at the 2:1 ratio beyond 5 mM. The **OTgCS** macrocycle was mixed with 0.5 equiv of the phenylene diphosphate monomer to achieve the 2:1 ratio for homopolymerization to form $(\mathbf{A})_n$. The diagnostic OH peak at 13.7 ppm indicates the presence of encapsulated phosphate−phosphate dimers in the supramolecular homopolymer $(\mathbf{A})_n$. Broad peaks (Figure 4b, middle) in the 7−9 ppm region, which do not match the sharp peaks (Figure 2c) seen in the homopolymer with the long flexible diphosphate $(\mathbf{C})_n$, instead suggest the formation of large aggregates. This interpretation is consistent with the small diffusion coefficient ($(1.0 \pm 0.2) \times 10^{-10}$ m^2/s, 5 mM) consistent with a 47-fold larger volume relative to the 2:2 model complex ($(3.7 \pm 0.1) \times 10^{-10}$ m^2/s, 5 mM).

Addition of slightly more diphosphate monomer (e.g., 0.7 equiv) leads to production of a more complicated spectrum (Figure S14) attributed to a species of intermediate sequence. We see decreasing intensity in peaks corresponding to the supramolecular polymer $(\mathbf{A})_n$ around 7.3 ppm (H_c) and the OH peak at 13.7 ppm. At the same time, a new species is produced represented by H_c peaks around 7.4 and 7.5 ppm as well as two OH peaks emerging at 14.3 and 14.6 ppm. These observations indicate that the encapsulated phosphate−phosphate dimers are in different chemical environments at this intermediate molar ratio. The sequences associated with this intermediate likely sit between those of the supramolecular homopolymer $(\mathbf{A})_n$ and copolymer $(\mathbf{AB})_n$.

In order to achieve the correct mole ratio to produce the alternating copolymer $(\mathbf{AB})_n$, we added 1.0 equiv of phenylene diphosphate. Clear cyanostar-based peaks characteristic of the 2:2 linkage chemistry, (**A**), were observed (Figure 4b, bottom). Again, the diffusion coefficient ($(1.2 \pm 0.1 \times 10^{-10})$ m^2/s) based on peaks in the aromatic region was much smaller than that of the 2:2 complex ($(3.7 \pm 0.1) \times 10^{-10}$ m^2/s), corresponding to a species that is 27-fold larger. The OH peak at 14.6 ppm confirms the phosphate−phosphate dimers are encapsulated inside the cyanostar dimers. The hydrogen-bonded OH protons of the uncomplexed phosphate−phosphate dimers cannot be identified from the ^{1}H NMR spectra. This finding is consistent with previous studies[71] involving complexation of dihydrogen phosphate $H_2PO_4^-$ dimers and trimers with **tBuCS**. Diagnostic of the alternating copolymer, the phenylene monomer's symmetry is broken and gives rise to two peaks of equal intensity at 6.5 and 6.4 ppm. (Figure S18). We also see two peaks in the ^{31}P NMR spectra (Figure S20). Consistently, we only see one resonance from the homopolymer $(\mathbf{A})_n$. The two different chemical environments coincide with the crystal packing structure of the alternating copolymer $(\mathbf{AB})_n$ (Figure 3).

Structural evidence for the alternating copolymer is provided from the ^{1}H−^{1}H NOESY correlations. First, we observe a cross-peak from the phenylene ring of the diphosphate monomer (Figure 5, H_1, H_2) to the protons (H_α) on the TBA^+ counter cations indicative of the ion-pairing interactions expected for the unencapsulated phosphate−phosphate dimers. These ion-pair interactions must be reasonably long-lived to generate NOE cross-peaks. This cross peak is not seen in the homopolymer $(\mathbf{A})_n$. Correlation peaks in the ^{1}H−^{1}H

https://dx.doi.org/10.1021/jacs.9b12645
J. Am. Chem. Soc. XXXX, XXX, XXX−XXX

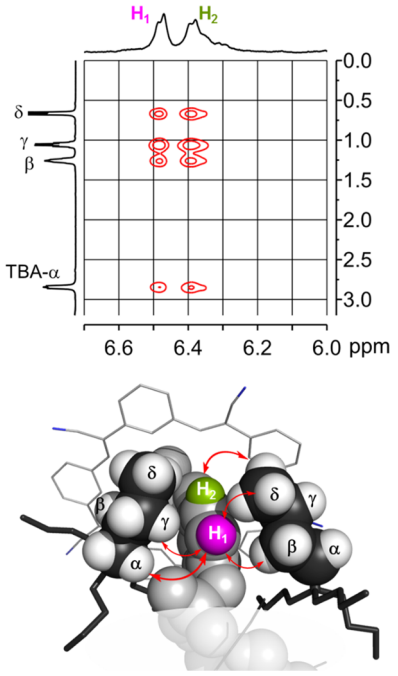

Figure 5. Partial ^{1}H−^{1}H NOESY spectra of the alternating copolymer shows correlations between TBA^+ cation and the phenylene diphosphate monomers ([**OTgCS**] = 5 mM, CD_2Cl_2, 298 K, 500 MHz).

NOESY plot (Figure S30) between the protons inside the macrocycle cavity (H_a, H_d) and on the phenylene diphosphate (OH, H_1, H_2) also support formation of the cyanostar-stabilized phosphate dimer. All these results are consistent with the two different forms of the phosphate−phosphate dimers in the alternating copolymer. If instead a random or statistical sequence was present, e.g., AABABBBA, we would expect a larger number of ^{1}H NMR peaks associated with the greater variety of chemical environments. As we only see two major peaks for the phenyl ring of the phenylene diphosphate in a 1:1 ratio, an alternating copolymer is supported.

To the best of our knowledge, this is the first time that stoichiometry has been shown to control the sequence of supramolecular polymers. We can plot the species variation as a function of stoichiometry using the signatures assigned to the homopolymer $(\mathbf{A})_n$ and alternating copolymer $(\mathbf{AB})_n$ (Figure 4c). For this speciation plot, we used a combination of the OH peaks and the aromatic peaks in the 7.0−7.6 ppm region to determine relative peak intensities (Figure S14). We also include the intermediate species by using the OH peak at 14.3. In the speciation curve (Figure 4c), we see the supramolecular homopolymer $(\mathbf{A})_n$ dominates at 2:1 stoichiometry (0.5 equiv) and the alternating copolymer $(\mathbf{AB})_n$ dominates at the 1:1 stoichiometry (1.0 equiv).

In order to understand the concentration-dependence for the stoichiometry-controlled supramolecular polymerization, we repeated the titrations at lower ([**OTgCS**] = 0.5 mM) and higher ([**OTgCS**] = 50 mM) concentrations (Figures S16 and S17). We see the distribution of species largely remains the same with increasing concentration.

Concentration-Driven Supramolecular Polymerization. Increasing the concentration of monomers is known to drive supramolecular polymerization. Consistently, diffusion NMR studies show the size of the both $(\mathbf{A})_n$ and $(\mathbf{AB})_n$ polymers undergo a 21-fold and 87-fold volume change from 1 mM to 50 mM, respectively (Figure 6a). For the phenylene diphosphate, however, diffusion coefficients show a small decrease indicating a 2.6-fold volume change consistent with a previous study for the dodecylene diphosphonate.[52] These results suggest that cyanostar-stabilized anion−anion dimers are responsible for the driving force of supramolecular polymerization. We also see the diffusion coefficients for the $(\mathbf{AB})_n$ copolymer becomes larger than $(\mathbf{A})_n$ at concentrations above 50 mM. This result is consistent with increased ion pairing helping to stabilize the uncomplexed phosphate−phosphate dimers at higher concentrations. We also see from these results that the diffusion coefficient of the **OTgCS** macrocycle decreases over this concentration range. This behavior is indicative of self-association facilitated by $\pi-\pi$ interactions between the faces of **OTgCS** macrocycles. Variable concentration studies followed by NMR spectroscopy show that this macrocycle aggregates more than the parent cyanostar consistent with the role of glycol chains in stabilizing self-associated stacks of shape-persistent macrocycles (Figure S9).[87,88]

To further verify the concentration-driven polymerization behavior, we conducted specific viscosity measurements (Figure 6b). The double-logarithmic plots of specific viscosity versus

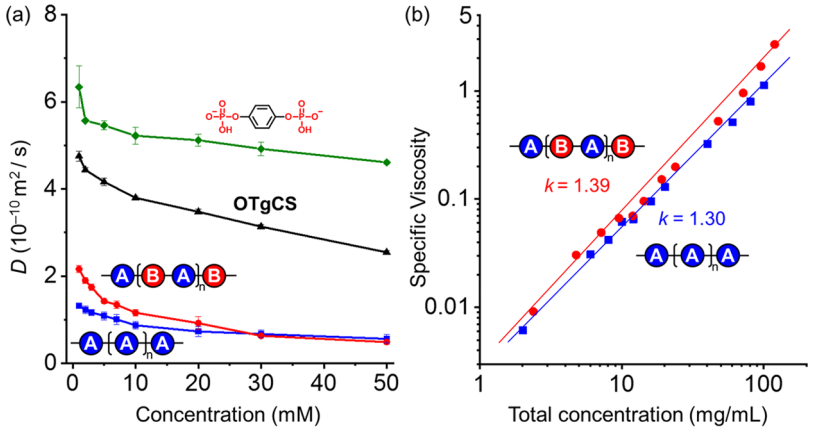

Figure 6. (a) Changes in diffusion coefficients of the phenylene diphosphate, **OTgCS**, homopolymer, and alternating copolymer with increasing concentration. (b) Specific viscosity of the homopolymer and the alternating copolymer versus concentration change in mg/mL (dichloromethane, 298 K, 600 MHz).

https://dx.doi.org/10.1021/jacs.9b12645
J. Am. Chem. Soc. XXXX, XXX, XXX−XXX

concentration for supramolecular polymers $(\mathbf{A})_n$ and $(\mathbf{AB})_n$ display slopes of 1.30 and 1.39, respectively. We see the alternating copolymer shows a slightly larger slope than the homopolymer suggesting the alternating copolymer is more likely to be physically entangled.[89] A turning point in these plots are sometimes observed and then assigned to the critical polymerization concentration (CPC).[90] The absence of such a point over the concentration range examined here suggests that $(\mathbf{A})_n$ and $(\mathbf{AB})_n$ are already above the CPC. This type of behavior has been seen previously in supramolecular polymers that were promoted by rigid monomers.[17,45]

Stoichiometry-Controlled Adhesion Properties of the Supramolecular Polymers. Structure−property relationships can be established by correlating the different supramolecular polymer sequences, $(\mathbf{A})_n$ and $(\mathbf{AB})_n$, to their adhesive properties. In contrast to the supramolecular polymer based on the parent macrocycle **tBuCS**, we did not observe precipitation when using **OTgCS** thereby allowing for further study of its bulk properties. The supramolecular polymers derived from **OTgCS** are sticky and viscous at high concentration. Inspired by this observation and other supramolecular polymer adhesives,[73] we hypothesized that the **OTgCS**-based supramolecular polymers could be used as adhesive materials. Specifically, for binding hydrophilic surfaces together (Figure 7a), such as glass, on account of OH···O hydrogen bonding from surface hydroxyls (SiOH) to the ether oxygens in the triethylene glycol chains of the **OTgCS** macrocycle (Figure 7b).[74,78]

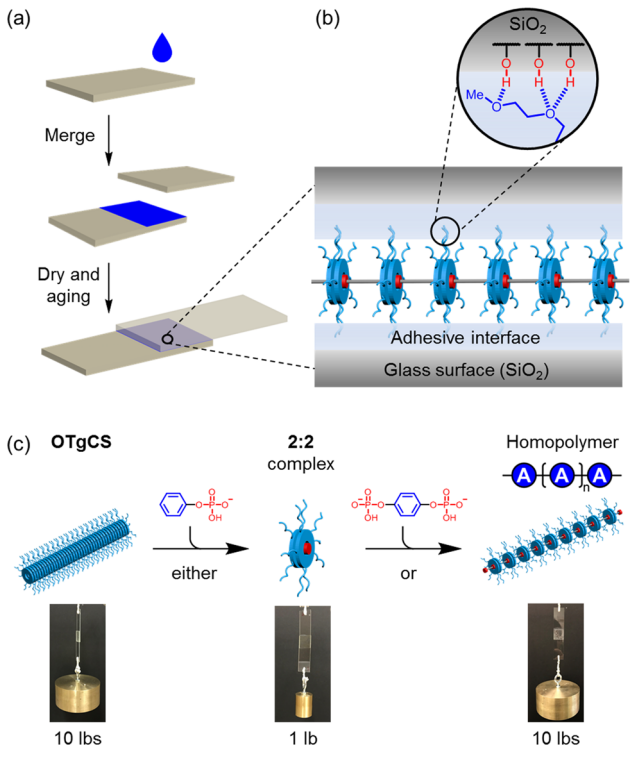

Figure 7. (a) Schematic procedure of preparing adhesive samples using glass slides. (b) Representation of the hydrogen bonding interaction between hydrophilic glass surface and the triethylene glycol chains from **OTgCS** macrocycles on the polymer. (c) Photographs showing adhesion behavior of **OTgCS**, the 2:2 complex of **OTgCS** and phenyl monophosphate, and the supramolecular homopolymer of $(\mathbf{A})_n$ using the phenylene diphosphate, respectively. Adhesive sample loading is 10 mg, and loading area is 2.5 × 2.5 cm^2.

Each supramolecular polymer was used to coat glass slides with a 2.5 × 2.5 cm^2 overlap area, and the resulting slides were used to support weights for initial adhesion testing (Figure 7c). We observed that the **OTgCS** macrocycle alone is capable of supporting a 10-lb weight (Figure 7c, left). This behavior is attributed to the self-aggregation of **OTgCS** macrocycles seen in the variable concentration studies monitored by diffusion NMR (Figure 6a) and ^{1}H NMR spectroscopies (Figure S9). Assuming the π-stacking between **OTgCS** macrocycles dominates the self-assembly, the triethylene glycol chains are free to interact with the hydrophilic surface through hydrogen bonding. Pull-off (Figure 8a) and lap-shear (Figure S35) adhesion tests were performed to quantify the adhesion strength of **OTgCS** (Table 1). The **OTgCS** macrocycle shows a strong pull-off tensile strength of 3.6 ± 0.4 MPa and a shear strength of 1.6 ± 0.6 MPa. For comparison, the **tBuCS** macrocycle did not display any adhesive properties, which supports the significant role of the triethylene glycol chains in adhesion.

For the small-molecule 2:2 complex between the **OTgCS** macrocycle and phenyl monophosphate, we observed very weak adhesion that only supported a 1-lb weight (Figure 7c, middle), with a pull-off adhesion strength of 0.5 ± 0.2 MPa and a shear strength of 0.2 ± 0.1 MPa (Table 1). The weaker adhesion strength is consistent with loss of macrocycle self-association upon complexation. This change from an associated state to a complex one has been seen with a related tricarbozole macrocycle that displays a high degree of self-association.[69] Thus, while the hydrogen bonding between the surface and the glycol chains is important for strong adhesion when using the **OTgCS** macrocycles, addition of the custom-designed organophosphate anions to drive formation of 2:2 complexes is insufficient to create an adhesive material.

Strong adhesion is expected from the supramolecular polymers where the 2:2 linkages are now covalently linked together. Consistently, we see the supramolecular homopolymer $(\mathbf{A})_n$ supports a 10-lb weight (Figure 7c, right), with a pull-off strength of 4.2 ± 0.4 MPa (Figure 8b). This adhesion strength is comparable to a supramolecular adhesive made using benzenetricarboxmide triply substituted with benzo-21-crown-7 (4.2 MPa),[74] which relies on hydrogen bonding linkages. By doing a single lap-shear test, we see the supramolecular homopolymer shows a shear strength (2.0 ± 0.5 MPa), which is comparable to a metal-coordination driven supramolecular copolymer based on poly(thioctic acid diisopropenylbenzene) (2.5 MPa).[78] It is clear from this performance that anion-driven supramolecular polymers display adhesion properties that match supramolecular polymers supported by more traditional linkage chemistries. Nevertheless, it is counterintuitive that the strong adhesion arises from linkage chemistry involving two like charges. These linkages are expected to repel each other and inhibit, instead of enhance, adhesion. The fact that this expectation is not fulfilled is remarkable and underscores the role of cyanostar recognition in helping reshape the terms of conventional wisdom.

In the case of the alternating copolymer $(\mathbf{AB})_n$, exactly half of the cyanostar-stabilized linkages are replaced by cation-stabilized linkages such that every other phosphate−phosphate dianion (2−) is stabilized by four proximal cations (4+). This system falls squarely in the realms of our conventional wisdom where the attraction between opposite charges is expected to contribute to significant stabilization in the solid state.

https://dx.doi.org/10.1021/jacs.9b12645
J. Am. Chem. Soc. XXXX, XXX, XXX−XXX

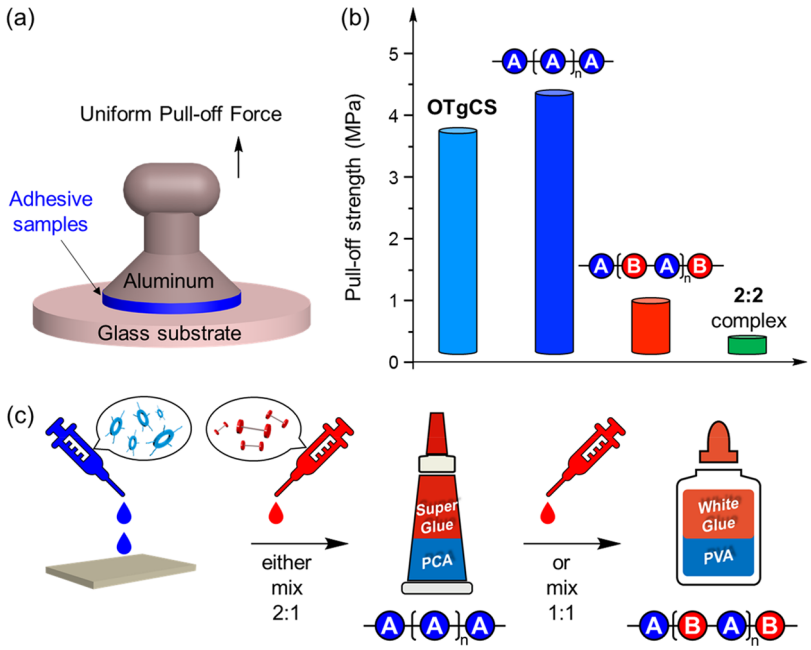

Figure 8. (a) Representation of the pull-off strength test for adhesive samples. (b) Pull-off strength of **OTgCS**, the 2:2 complex between **OTgCS** and phenyl monophosphate, the supramolecular homopolymer $(\mathbf{A})_n$, and the copolymer $(\mathbf{AB})_n$ using the phenylene diphosphate. (c) Representation of tunable supramolecular polymer adhesives made from a two-pot mix into either the superglue grade homopolymer or white glue grade copolymer.

Table 1. Quantitative Adhesion Strength of Supramolecular Polymers, Control Monomers, 2:2 Complex, Commercial Glues, and Other Supramolecular Polymer Adhesives[a]

Sample	Pull-off strength (MPa)	Lap-shear strength (MPa)
OTgCS	3.6 ± 0.4	1.6 ± 0.6
2:2 complex	0.5 ± 0.2	0.2 ± 0.1
$(\mathbf{A})_n$	4.2 ± 0.4	2.0 ± 0.5
$(\mathbf{AB})_n$	0.9 ± 0.2	0.4 ± 0.2
$(\mathbf{C})_n$	2.4 ± 0.3	1.1 ± 0.2
Superglue	5–9	–
White glue	0.4	–
Hydrogen bonding driven SPs[b]	4.2	–
Metal-coordination SPs[c]	–	2.5

[a]Sample loading of tested materials is about 10 mg, loading area is 2.5 × 2.5 cm^2. [b]Hydrogen bonding driven supramolecular polymer using triply benzo-21-crown-7-substituted 1,3,5-benzenetricarboxamides.[74] [c]Metal-coordination driven supramolecular polymer based on iron coordinated poly(thioctic acid diisopropenylbenzene).[78]

Furthermore, solids typically support closer contacts and lower dielectric constants than solutions. From Coulomb's law, therefore, this ionic bonding is expected to be substantial. It is not clear *a priori*, therefore, if the bulk samples of the homopolymer $(\mathbf{A})_n$ or the copolymer $(\mathbf{AB})_n$ would have stronger adhesion.

A much weaker adhesion strength was observed for the alternating supramolecular copolymer $(\mathbf{AB})_n$ than the homopolymer $(\mathbf{A})_n$. A pull-off strength of 0.9 ± 0.2 MPa and a shear strength of 0.4 ± 0.2 MPa were observed (Figure 8b). The copolymer displays only about 20% the adhesion strength of the homopolymer. This observation strongly suggests that the linkage defined by cyanostar-stabilized *anti*-electrostatic phosphate dimers is stronger than that defined by the cation-stabilized phosphate dimers.

To provide further support for the roles of cyanostar-stabilized and cation-stabilized anion–anion linkages, we conducted a series of control studies. To enhance the electrostatic driving force, we added extra TBA^+ salts and consistently saw increases in the adhesion strength (Figure S32) of the alternating copolymer. To test for the role of the cyanostar in adhesion, we evaluated a neat film of the phenylene diphosphate monomer alone. No adhesion was observed, which is attributed to the absence of surface-active glycols. To emulate the surface interaction, we mixed the rigid monomer with 1 equiv of polyethylene glycol of a molecular weight (M_w = 2000 g mol^{-1}) matching the two cyanostars used in homopolymer $(\mathbf{A})_n$. No adhesion was observed in this case either (Figure S33). These results support the finding that the anion–anion linkages also benefit substantially from cyanostar stabilization. We evaluated the adhesion strength (Table 1) of the supramolecular polymer $(\mathbf{C})_n$ composed of the flexible triethylene glycol bis(phenyl-*p*-phosphate) and found it is about half that of $(\mathbf{A})_n$ despite having the same amount of cyanostar in each case. This result suggests that the compact character of the supramolecular polymer chain in $(\mathbf{A})_n$ provides better support for adhesion.

Reversible and Tunable Adhesion. The adhesion properties of the supramolecular homopolymer $(\mathbf{A})_n$ are thermally reversible. A 10-lb weight was released by external heating (~50–60 °C) of the bonded glass slides for ~30 s (Figure S34). We observe that both faces of the debonded glass slides retain some of the supramolecular adhesive material indicating that the debonding occurred within the adhesive material. This heat-induced debonding can be attributed to either the loss of physical entanglement mediated by the glycol chains on the **OTgCS** macrocycles and/or the dissociation of the 2:2 supramolecular linkages upon heating. The adhesion strength could be recovered by overlapping the two slides together and storing them under vacuum for 1 h. Presumably,

https://dx.doi.org/10.1021/jacs.9b12645
J. Am. Chem. Soc. XXXX, XXX, XXX–XXX

the supramolecular polymer is able to dynamically reform at the physically contacted interface. This reversible process could be repeated for a few cycles without losing the base adhesion strength.

On account of the dynamic and stimuli-responsive characteristics of supramolecular linkages, the reusability[91−93] we showed here or interfacial self-healing properties[14,94,95] are typical features of supramolecular polymer adhesives. However, to the best of our knowledge, this is the first report that demonstrates a supramolecular polymer with tunable adhesion strength based on controlling the polymer sequence (Figure 8c). Specifically, the homopolymer $(\mathbf{A})_n$ shows comparable adhesion strength to commercial superglue formulations based on polycyanoacrylate (5−9 MPa, Table 1),[73] while the adhesion strength of the copolymer $(\mathbf{AB})_n$ is comparable to white glue based on poly(vinyl acetate) (0.43 MPa, Table 1).[74] Thus, we can tune the adhesion strength of the supramolecular polymer between that of superglue and white glue simply by changing the stoichiometric ratio of the monomers (Figure 8c). Consistently, we also see an intermediate mixture of cyanostar with 0.75 equiv of phenylene diphosphate shows a 2.1 ± 0.3 MPa pull-off strength and 0.9 ± 0.2 MPa lap-shear strength. The properties stem directly from the sequence-defined structures and the strengths of the supramolecular linkage chemistries. This study provides a new way to understand how material properties reflect structural information in the form of anion-driven supramolecular polymer adhesives.

CONCLUSIONS

We discovered a new form of sequence control in supramolecular polymers based on diphosphate monomers of compact size mixed with cyanostar macrocycles to drive phosphate−phosphate dimerization. With a 2:1 stoichiometry, a supramolecular homopolymer $(\mathbf{A})_n$ is produced that is composed of phosphate−phosphate dimers inside π-stacked cyanostar macrocycles. At a 1:1 stoichiometry, the alternating supramolecular copolymer $(\mathbf{AB})_n$ is codriven by cyanostar-stabilized phosphate dimers and cation-stabilized phosphate dimers. The cation-stabilized dimers emerge hierarchically from the superstructure in which the stronger primary cyanostar-stabilized linkages liberate extra cations that are used to reinforce the secondary ionic linkage. The two types of anion−anion dimers constitute orthogonal linkage chemistries, which are required to elicit sequence control. This study further demonstrates the utility of anion−anion dimerization to synthesize functional and tunable supramolecular polymers. This is the first time that these linkages have been transformed into a polymer capable of supporting materials properties expressed here as adhesion. The supramolecular homopolymer $(\mathbf{A})_n$ displays strong adhesive properties, whereas the alternating supramolecular copolymer $(\mathbf{AB})_n$ has less adhesion strength. Here we see expression of the remarkable idea that the sum of attractive driving forces in the anion−anion linkages overcomes their repulsions when stabilized by complementary cyanostar receptors to a greater extent than traditional ionic contacts. Thus, the adhesion strength of the supramolecular polymers is composition-dependent, which corresponds directly to the stoichiometry- and sequenced-controlled state of polymerization. We believe that this study lays a foundation for a broad variety of anion-based materials with customized properties derived from custom-designed anions and helps to expand the scope of anion-relevant supramolecular systems.

ASSOCIATED CONTENT

Supporting Information

The Supporting Information is available free of charge at https://pubs.acs.org/doi/10.1021/jacs.9b12645.

General methods, synthetic procedures, crystallography, ^{1}H NMR titrations, 2D NMR analysis, diffusion NMR studies, viscosity measurement, weight-lifting test, ^{1}H and ^{13}C NMR characterizations (PDF)

Crystallographic data for **tBuCS** and Phenylene Disphosphate·2TBA (CIF)

AUTHOR INFORMATION

Corresponding Author

Amar H. Flood − *Department of Chemistry, Indiana University, Bloomington, Indiana 47405, United States;* orcid.org/0000-0002-2764-9155; Email: aflood@indiana.edu

Authors

Wei Zhao − *Department of Chemistry, Indiana University, Bloomington, Indiana 47405, United States*

Joshua Tropp − *School of Polymer Science and Engineering, The University of Southern Mississippi, Hattiesburg, Mississippi 39406, United States*

Bo Qiao − *Department of Chemistry, Indiana University, Bloomington, Indiana 47405, United States*

Maren Pink − *Department of Chemistry, Indiana University, Bloomington, Indiana 47405, United States*

Jason D. Azoulay − *School of Polymer Science and Engineering, The University of Southern Mississippi, Hattiesburg, Mississippi 39406, United States;* orcid.org/0000-0003-0138-5961

Complete contact information is available at: https://pubs.acs.org/10.1021/jacs.9b12645

Notes

The authors declare no competing financial interest.

ACKNOWLEDGMENTS

A.H.F. acknowledges support from the National Science Foundation (CHE 1709909). J.D.A. acknowledges support from the National Science Foundation (OIA 1632825). J.T. acknowledges traineeship support from the NSF NRT program "Interface" (DGE 1449999) through the University of Southern Mississippi.

REFERENCES

(1) Yanagisawa, Y.; Nan, Y.; Okuro, K.; Aida, T. Mechanically robust, readily repairable polymers via tailored noncovalent cross-linking. *Science* **2018**, *359*, 72.

(2) Gu, Y.; Alt, E. A.; Wang, H.; Li, X.; Willard, A. P.; Johnson, J. A. Photoswitching topology in polymer networks with metal−organic cages as crosslinks. *Nature* **2018**, *560*, 65.

(3) Brunsveld, L.; Folmer, B.; Meijer, E. W.; Sijbesma, R. Supramolecular polymers. *Chem. Rev.* **2001**, *101*, 4071.

(4) Dankers, P. Y.; Harmsen, M. C.; Brouwer, L. A.; Van Luyn, M. J.; Meijer, E. A modular and supramolecular approach to bioactive scaffolds for tissue engineering. *Nat. Mater.* **2005**, *4*, 568.

(5) Aida, T.; Meijer, E.; Stupp, S. Functional supramolecular polymers. *Science* **2012**, *335*, 813.

(6) Lutz, J.-F.; Lehn, J.-M.; Meijer, E.; Matyjaszewski, K. From precision polymers to complex materials and systems. *Nat. Rev. Mater.* **2016**, *1*, 16024.

(7) Vantomme, G.; Meijer, E. The construction of supramolecular systems. *Science* **2019**, *363*, 1396.

(8) Lehn, J. M. Perspectives in supramolecular chemistry—from molecular recognition towards molecular information processing and self-organization. *Angew. Chem., Int. Ed. Engl.* **1990**, *29*, 1304.
(9) Lehn, J.-M. From supramolecular chemistry towards constitutional dynamic chemistry and adaptive chemistry. *Chem. Soc. Rev.* **2007**, *36*, 151.
(10) Webber, M. J.; Appel, E. A.; Meijer, E.; Langer, R. Supramolecular biomaterials. *Nat. Mater.* **2016**, *15*, 13.
(11) Zou, L.; Braegelman, A. S.; Webber, M. J. Spatially Defined Drug Targeting by in Situ Host−Guest Chemistry in a Living Animal. *ACS Cent. Sci.* **2019**, *5*, 1035.
(12) Li, C.-H.; Wang, C.; Keplinger, C.; Zuo, J.-L.; Jin, L.; Sun, Y.; Zheng, P.; Cao, Y.; Lissel, F.; Linder, C.; You, X.-Z.; Bao, Z. A highly stretchable autonomous self-healing elastomer. *Nat. Chem.* **2016**, *8*, 618.
(13) Choi, S.; Kwon, T.-w.; Coskun, A.; Choi, J. W. Highly elastic binders integrating polyrotaxanes for silicon microparticle anodes in lithium ion batteries. *Science* **2017**, *357*, 279.
(14) Ji, X.; Wu, R. T.; Long, L.; Ke, X. S.; Guo, C.; Ghang, Y. J.; Lynch, V. M.; Huang, F.; Sessler, J. L. Encoding, Reading, and Transforming Information Using Multifluorescent Supramolecular Polymeric Hydrogels. *Adv. Mater.* **2018**, *30*, 1705480.
(15) Burnworth, M.; Tang, L.; Kumpfer, J. R.; Duncan, A. J.; Beyer, F. L.; Fiore, G. L.; Rowan, S. J.; Weder, C. Optically healable supramolecular polymers. *Nature* **2011**, *472*, 334.
(16) Lutz, J.-F.; Ouchi, M.; Liu, D. R.; Sawamoto, M. Sequence-controlled polymers. *Science* **2013**, *341*, 1238149.
(17) Wei, P.; Yan, X.; Cook, T. R.; Ji, X.; Stang, P. J.; Huang, F. Supramolecular Copolymer Constructed by Hierarchical Self-Assembly of Orthogonal Host-Guest, H-Bonding, and Coordination Interactions. *ACS Macro Lett.* **2016**, *5*, 671.
(18) Wei, P.; Yan, X.; Huang, F. Supramolecular polymers constructed by orthogonal self-assembly based on host−guest and metal−ligand interactions. *Chem. Soc. Rev.* **2015**, *44*, 815.
(19) Yan, X.; Cook, T. R.; Pollock, J. B.; Wei, P.; Zhang, Y.; Yu, Y.; Huang, F.; Stang, P. J. Responsive supramolecular polymer metallogel constructed by orthogonal coordination-driven self-assembly and host/guest interactions. *J. Am. Chem. Soc.* **2014**, *136*, 4460.
(20) Wang, F.; Han, C.; He, C.; Zhou, Q.; Zhang, J.; Wang, C.; Li, N.; Huang, F. Self-sorting organization of two heteroditopic monomers to supramolecular alternating copolymers. *J. Am. Chem. Soc.* **2008**, *130*, 11254.
(21) Kim, D. S.; Chang, J.; Leem, S.; Park, J. S.; Thordarson, P.; Sessler, J. L. Redox-and pH-Responsive Orthogonal Supramolecular Self-Assembly: An Ensemble Displaying Molecular Switching Characteristics. *J. Am. Chem. Soc.* **2015**, *137*, 16038.
(22) Zeng, F.; Han, Y.; Chen, C.-F. Self-sorting behavior of a four-component host−guest system and its incorporation into a linear supramolecular alternating copolymer. *Chem. Commun.* **2015**, *51*, 3593.
(23) Besenius, P. Controlling supramolecular polymerization through multicomponent self-assembly. *J. Polym. Sci., Part A: Polym. Chem.* **2017**, *55*, 34.
(24) Li, H.; Fan, X.; Min, X.; Qian, Y.; Tian, W. Controlled Supramolecular Architecture Transformation from Homopolymer to Copolymer through Competitive Self-Sorting Method. *Macromol. Rapid Commun.* **2017**, *38*, 1600631.
(25) Chakraborty, S.; Ray, D.; Aswal, V. K.; Ghosh, S. Multi-Stimuli-Responsive Directional Assembly of an Amphiphilic Donor−Acceptor Alternating Supramolecular Copolymer. *Chem. - Eur. J.* **2018**, *24*, 16379.
(26) Nadamoto, K.; Maruyama, K.; Fujii, N.; Ikeda, T.; Kihara, S. i.; Haino, T. Supramolecular Copolymerization by Sequence Reorganization of a Supramolecular Homopolymer. *Angew. Chem., Int. Ed.* **2018**, *57*, 7028.
(27) Hirao, T.; Kudo, H.; Amimoto, T.; Haino, T. Sequence-controlled supramolecular terpolymerization directed by specific molecular recognitions. *Nat. Commun.* **2017**, *8*, 634.
(28) Raeisi, M.; Kotturi, K.; del Valle, I.; Schulz, J.; Dornblut, P.; Masson, E. Sequence-Specific Self-Assembly of Positive and Negative Monomers with Cucurbit[8]uril Linkers. *J. Am. Chem. Soc.* **2018**, *140*, 3371.
(29) Shi, X.; Zhang, X.; Ni, X.-L.; Zhang, H.; Wei, P.; Liu, J.; Xing, H.; Peng, H.-Q.; Lam, J. W.; Zhang, P. Supramolecular Polymerization with Dynamic Self-Sorting Sequence Control. *Macromolecules* **2019**, *52*, 8814.
(30) Wang, X.; Han, K.; Li, J.; Jia, X.; Li, C. Pillar[5]arene−neutral guest recognition based supramolecular alternating copolymer containing [c2] daisy chain and bis-pillar[5]arene units. *Polym. Chem.* **2013**, *4*, 3998.
(31) Felder, T.; de Greef, T. F.; Nieuwenhuizen, M. M.; Sijbesma, R. P. Alternation and tunable composition in hydrogen bonded supramolecular copolymers. *Chem. Commun.* **2014**, *50*, 2455.
(32) Ahmed, S.; Singha, N.; Pramanik, B.; Mondal, J. H.; Das, D. Redox controlled reversible transformation of a supramolecular alternating copolymer to a radical cation containing homo-polymer. *Polym. Chem.* **2016**, *7*, 4393.
(33) Chakraborty, S.; Kar, H.; Sikder, A.; Ghosh, S. Steric ploy for alternating donor−acceptor co-assembly and cooperative supramolecular polymerization. *Chem. Sci.* **2017**, *8*, 1040.
(34) He, Z.; Jiang, W.; Schalley, C. A. Integrative self-sorting: a versatile strategy for the construction of complex supramolecular architecture. *Chem. Soc. Rev.* **2015**, *44*, 779.
(35) Adelizzi, B.; Van Zee, N. J.; de Windt, L. N.; Palmans, A. R.; Meijer, E. W. Future of supramolecular copolymers unveiled by reflecting on covalent copolymerization. *J. Am. Chem. Soc.* **2019**, *141*, 6110.
(36) Complementary names for the homopolymer and alternating copolymer are poly(pseudo rotaxane) and poly(pseudo rotaxane) with a periodically defined location of the ring parts, respectively.
(37) Lee, J.; Ghosh, K.; Stang, P. J. Stoichiometric control of multiple different tectons in coordination-driven self-assembly: preparation of fused metallacyclic polygons. *J. Am. Chem. Soc.* **2009**, *131*, 12028.
(38) D'Urso, A.; Cristaldi, D. A.; Fragalà, M. E.; Gattuso, G.; Pappalardo, A.; Villari, V.; Micali, N.; Pappalardo, S.; Parisi, M. F.; Purrello, R. Sequence, Stoichiometry, and Dimensionality Control in Porphyrin/Bis-calix[4]arene Self-Assemblies in Aqueous Solution. *Chem. - Eur. J.* **2010**, *16*, 10439.
(39) Lin, C.; Xu, L.; Huang, L.; Chen, J.; Liu, Y.; Ma, Y.; Ye, F.; Qiu, H.; He, T.; Yin, S. Metal Coordination Stoichiometry Controlled Formation of Linear and Hyperbranched Supramolecular Polymers. *Macromol. Rapid Commun.* **2016**, *37*, 1453.
(40) Wang, F.; Feng, C. L. Stoichiometry-Controlled Inversion of Supramolecular Chirality in Nanostructures Co-assembled with Bipyridines. *Chem. - Eur. J.* **2018**, *24*, 1509.
(41) Ji, W.; Yuan, C.; Chakraborty, P.; Gilead, S.; Yan, X.; Gazit, E. Stoichiometry-controlled secondary structure transition of amyloid-derived supramolecular dipeptide co-assemblies. *Commun. Chem.* **2019**, *2*, 65.
(42) Li, P.; Lü, B.; Han, D.; Duan, P.; Liu, M.; Yin, M. Stoichiometry-controlled inversion of circularly polarized luminescence in co-assembly of chiral gelators with an achiral tetraphenylethylene derivative. *Chem. Commun.* **2019**, *55*, 2194.
(43) Gong, H.-Y.; Rambo, B. M.; Karnas, E.; Lynch, V. M.; Sessler, J. L. A 'Texas-sized'molecular box that forms an anion-induced supramolecular necklace. *Nat. Chem.* **2010**, *2*, 406.
(44) Whittell, G. R.; Hager, M. D.; Schubert, U. S.; Manners, I. Functional soft materials from metallopolymers and metallosupramolecular polymers. *Nat. Mater.* **2011**, *10*, 176.
(45) Scherman, O. A.; Ligthart, G.; Sijbesma, R. P.; Meijer, E. A Selectivity-Driven Supramolecular Polymerization of an AB Monomer. *Angew. Chem., Int. Ed.* **2006**, *45*, 2072.
(46) Qin, B.; Zhang, S.; Song, Q.; Huang, Z.; Xu, J. F.; Zhang, X. Supramolecular Interfacial Polymerization: A Controllable Method of Fabricating Supramolecular Polymeric Materials. *Angew. Chem., Int. Ed.* **2017**, *56*, 7639.

https://dx.doi.org/10.1021/jacs.9b12645
J. Am. Chem. Soc. XXXX, XXX, XXX−XXX

(47) Ogi, S.; Sugiyasu, K.; Manna, S.; Samitsu, S.; Takeuchi, M. Living supramolecular polymerization realized through a biomimetic approach. *Nat. Chem.* **2014**, *6*, 188.
(48) Weingarten, A. S.; Kazantsev, R. V.; Palmer, L. C.; McClendon, M.; Koltonow, A. R.; Samuel, A. P.; Kiebala, D. J.; Wasielewski, M. R.; Stupp, S. I. Self-assembling hydrogel scaffolds for photocatalytic hydrogen production. *Nat. Chem.* **2014**, *6*, 964.
(49) Dong, S.; Luo, Y.; Yan, X.; Zheng, B.; Ding, X.; Yu, Y.; Ma, Z.; Zhao, Q.; Huang, F. A dual-responsive supramolecular polymer gel formed by crown ether based molecular recognition. *Angew. Chem., Int. Ed.* **2011**, *50*, 1905.
(50) Chen, H.; Huang, Z.; Wu, H.; Xu, J. F.; Zhang, X. Supramolecular Polymerization Controlled through Kinetic Trapping. *Angew. Chem., Int. Ed.* **2017**, *56*, 16575.
(51) McDonald, K. P.; Qiao, B.; Twum, E. B.; Lee, S.; Gamache, P. J.; Chen, C.-H.; Yi, Y.; Flood, A. H. Quantifying chloride binding and salt extraction with poly(methyl methacrylate) copolymers bearing aryl-triazoles as anion receptor side chains. *Chem. Commun.* **2014**, *50*, 13285.
(52) Zhao, W.; Qiao, B.; Tropp, J.; Pink, M.; Azoulay, J. D.; Flood, A. H. Linear Supramolecular Polymers Driven by Anion−Anion Dimerization of Difunctional Phosphonate Monomers Inside Cyanostar Macrocycles. *J. Am. Chem. Soc.* **2019**, *141*, 4980.
(53) Capici, C.; Cohen, Y.; D'Urso, A.; Gattuso, G.; Notti, A.; Pappalardo, A.; Pappalardo, S.; Parisi, M. F.; Purrello, R.; Slovak, S. Anion-Assisted Supramolecular Polymerization: From Achiral AB-Type Monomers to Chiral Assemblies. *Angew. Chem., Int. Ed.* **2011**, *50*, 11956.
(54) Rostami, A.; Wei, C. J.; Guérin, G.; Taylor, M. S. Anion Detection by a Fluorescent Poly (squaramide): Self-Assembly of Anion-Binding Sites by Polymer Aggregation. *Angew. Chem., Int. Ed.* **2011**, *50*, 2059.
(55) Gong, H.-Y.; Rambo, B. M.; Lynch, V. M.; Keller, K. M.; Sessler, J. L. Texas-Sized" Molecular Boxes: Building Blocks for the Construction of Anion-Induced Supramolecular Species via Self-Assembly. *J. Am. Chem. Soc.* **2013**, *135*, 6330.
(56) Silver, E. S.; Rambo, B. M.; Bielawski, C. W.; Sessler, J. L. Reversible Anion-Induced Cross-Linking of Well-Defined Calix[4]-pyrrole-Containing Copolymers. *J. Am. Chem. Soc.* **2014**, *136*, 2252.
(57) Zhang, Z.; Kim, D. S.; Lin, C.-Y.; Zhang, H.; Lammer, A. D.; Lynch, V. M.; Popov, I.; Miljanic′, O. S.; Anslyn, E. V.; Sessler, J. L. Expanded porphyrin-anion supramolecular assemblies: environmentally responsive sensors for organic solvents and anions. *J. Am. Chem. Soc.* **2015**, *137*, 7769.
(58) Tepper, R.; Bode, S.; Geitner, R.; Jäger, M.; Görls, H.; Vitz, J.; Dietzek, B.; Schmitt, M.; Popp, J.; Hager, M. D. Polymeric Halogen-Bond-Based Donor Systems Showing Self-Healing Behavior in Thin Films. *Angew. Chem., Int. Ed.* **2017**, *56*, 4047.
(59) Zapata, F.; González, L.; Caballero, A.; Bastida, A.; Bautista, D.; Molina, P. Interlocked Supramolecular Polymers Created by Combination of Halogen- and Hydrogen-Bonding Interactions through Anion-Template Self-Assembly. *J. Am. Chem. Soc.* **2018**, *140*, 2041.
(60) Weinhold, F.; Klein, R. A. Anti-Electrostatic Hydrogen Bonds. *Angew. Chem., Int. Ed.* **2014**, *53*, 11214.
(61) Frenking, G.; Caramori, G. F. No Need for a Re-examination of the Electrostatic Notation of the Hydrogen Bonding: A Comment. *Angew. Chem., Int. Ed.* **2015**, *54*, 2596.
(62) Mata, I.; Molins, E.; Alkorta, I.; Espinosa, E. The Paradox of Hydrogen-Bonded Anion−Anion Aggregates in Oxoanions: A Fundamental Electrostatic Problem Explained in Terms of Electrophilic···Nucleophilic Interactions. *J. Phys. Chem. A* **2015**, *119*, 183.
(63) Weinhold, F.; Klein, R. A. Improved General Understanding of the Hydrogen-Bonding Phenomena: A Reply. *Angew. Chem., Int. Ed.* **2015**, *54*, 2600.
(64) Knorr, A.; Stange, P.; Fumino, K.; Weinhold, F.; Ludwig, R. Spectroscopic Evidence for Clusters of Like-Charged Ions in Ionic Liquids Stabilized by Cooperative Hydrogen Bonding. *ChemPhysChem* **2016**, *17*, 458.
(65) Cullen, D. A.; Gardiner, M. G.; White, N. G. A three dimensional hydrogen bonded organic framework assembled through antielectrostatic hydrogen bonds. *Chem. Commun.* **2019**, *55*, 12020.
(66) White, N. G. Antielectrostatically hydrogen bonded anion dimers: counter-intuitive, common and consistent. *CrystEngComm* **2019**, *21*, 4855.
(67) Fatila, E. M.; Twum, E. B.; Sengupta, A.; Pink, M.; Karty, J. A.; Raghavachari, K.; Flood, A. H. Anions Stabilize Each Other inside Macrocyclic Hosts. *Angew. Chem., Int. Ed.* **2016**, *55*, 14057.
(68) Fatila, E. M.; Twum, E. B.; Karty, J. A.; Flood, A. H. Ion-pairing and Co-facial Stacking Drive High-fidelity Bisulfate Assembly with Cyanostar Macrocyclic Hosts. *Chem. - Eur. J.* **2017**, *23*, 10652.
(69) Dobscha, J. R.; Debnath, S.; Fadler, R. E.; Fatila, E. M.; Pink, M.; Raghavachari, K.; Flood, A. H. Host-host Interactions Control Self-assembly and Switching of Triple and Double Decker Stacks of Tricarbazole Macrocycles Co-assembled with *Anti*-electrostatic Bisulfate Dimers. *Chem. - Eur. J.* **2018**, *24*, 9841.
(70) Zhao, W.; Qiao, B.; Chen, C. H.; Flood, A. H. High-Fidelity Multistate Switching with Anion−Anion and Acid−Anion Dimers of Organophosphates in Cyanostar Complexes. *Angew. Chem., Int. Ed.* **2017**, *56*, 13083.
(71) Fatila, E. M.; Pink, M.; Twum, E. B.; Karty, J. A.; Flood, A. H. Phosphate-phosphate oligomerization drives higher order co-assemblies with stacks of cyanostar macrocycles. *Chem. Sci.* **2018**, *9*, 2863.
(72) Lee, S.; Chen, C.-H.; Flood, A. H. A pentagonal cyanostar macrocycle with cyanostilbene CH donors binds anions and forms dialkylphosphate [3]rotaxanes. *Nat. Chem.* **2013**, *5*, 704.
(73) Heinzmann, C.; Weder, C.; de Espinosa, L. M. Supramolecular polymer adhesives: advanced materials inspired by nature. *Chem. Soc. Rev.* **2016**, *45*, 342.
(74) Dong, S.; Leng, J.; Feng, Y.; Liu, M.; Stackhouse, C. J.; Schönhals, A.; Chiappisi, L.; Gao, L.; Chen, W.; Shang, J. Structural water as an essential comonomer in supramolecular polymerization. *Sci. Adv.* **2017**, *3*, eaao0900.
(75) Gebbie, M. A.; Wei, W.; Schrader, A. M.; Cristiani, T. R.; Dobbs, H. A.; Idso, M.; Chmelka, B. F.; Waite, J. H.; Israelachvili, J. N. Tuning underwater adhesion with cation−π interactions. *Nat. Chem.* **2017**, *9*, 473.
(76) Li, J.; Celiz, A.; Yang, J.; Yang, Q.; Wamala, I.; Whyte, W.; Seo, B.; Vasilyev, N.; Vlassak, J.; Suo, Z. Tough adhesives for diverse wet surfaces. *Science* **2017**, *357*, 378.
(77) Liu, J.; Tan, C. S. Y.; Scherman, O. A. Dynamic Interfacial Adhesion through Cucurbit[n]uril Molecular Recognition. *Angew. Chem., Int. Ed.* **2018**, *57*, 8854.
(78) Zhang, Q.; Shi, C.-Y.; Qu, D.-H.; Long, Y.-T.; Feringa, B. L.; Tian, H. Exploring a naturally tailored small molecule for stretchable, self-healing, and adhesive supramolecular polymers. *Sci. Adv.* **2018**, *4*, eaat8192.
(79) Saiz-Poseu, J.; Mancebo-Aracil, J.; Nador, F.; Busqué, F.; Ruiz-Molina, D. The Chemistry behind Catechol-Based Adhesion. *Angew. Chem., Int. Ed.* **2019**, *58*, 696.
(80) Zhang, Q.; Li, T.; Duan, A.; Dong, S.; Zhao, W.; Stang, P. J. Formation of a Supramolecular Polymeric Adhesive via Water-Participant Hydrogen Bonding Formation. *J. Am. Chem. Soc.* **2019**, *141*, 8058.
(81) Liu, Y.; Singharoy, A.; Mayne, C. G.; Sengupta, A.; Raghavachari, K.; Schulten, K.; Flood, A. H. Flexibility Coexists with Shape-Persistence in Cyanostar Macrocycles. *J. Am. Chem. Soc.* **2016**, *138*, 4843.
(82) Sheetz, E. G.; Qiao, B.; Pink, M.; Flood, A. H. Programmed Negative Allostery with Guest-Selected Rotamers Control Anion−Anion Complexes of Stackable Macrocycles. *J. Am. Chem. Soc.* **2018**, *140*, 7773.
(83) Gerasimchuk, O. A.; Mason, S.; Llinares, J. M.; Song, M.; Alcock, N. W.; Bowman-James, K. Binding of phosphate with a simple hexaaza polyammonium macrocycle. *Inorg. Chem.* **2000**, *39*, 1371.
(84) Němec, I.; Macháčková, Z.; Teubner, K.; Císařová, I.; Vaněk, P.; Mička, Z. The structural phase transitions of aminoguanidinium

https://dx.doi.org/10.1021/jacs.9b12645
J. Am. Chem. Soc. XXXX, XXX, XXX−XXX

(1+) dihydrogen phosphate−study of crystal structures, vibrational spectra and thermal behavior. *J. Solid State Chem.* **2004**, *177*, 4655.
(85) Dhara, A.; Flood, A. H. Cages Driven Away from Equilibrium Binding by Electric Fields. *Chem.* **2019**, *5*, 1017.
(86) Borsley, S.; Haugland, M. M.; Oldknow, S.; Cooper, J. A.; Burke, M. J.; Scott, A.; Grantham, W.; Vallejo, J.; Brechin, E. K.; Lusby, P. J. Electrostatic forces in field-perturbed equilibria: nanopore analysis of cage complexes. *Chem.* **2019**, *5*, 1275.
(87) Zhang, J.; Pesak, D. J.; Ludwick, J. L.; Moore, J. S. Geometrically-controlled and site-specifically-functionalized phenylacetylene macrocycles. *J. Am. Chem. Soc.* **1994**, *116*, 4227.
(88) Li, Y.; Flood, A. H. Strong, Size-Selective, and Electronically Tunable C−H···Halide Binding with Steric Control over Aggregation from Synthetically Modular, Shape-Persistent $[3_4]$Triazolophanes. *J. Am. Chem. Soc.* **2008**, *130*, 12111.
(89) Niu, Z.; Huang, F.; Gibson, H. W. Supramolecular AA−BB-type linear polymers with relatively high molecular weights via the self-assembly of bis (m-phenylene)-32-crown-10 cryptands and a bisparaquat derivative. *J. Am. Chem. Soc.* **2011**, *133*, 2836.
(90) Yang, L.; Tan, X.; Wang, Z.; Zhang, X. Supramolecular polymers: historical development, preparation, characterization, and functions. *Chem. Rev.* **2015**, *115*, 7196.
(91) Heinzmann, C.; Coulibaly, S.; Roulin, A.; Fiore, G. L.; Weder, C. Light-induced bonding and debonding with supramolecular adhesives. *ACS Appl. Mater. Interfaces* **2014**, *6*, 4713.
(92) Michal, B. T.; Spencer, E. J.; Rowan, S. J. Stimuli-responsive reversible two-level adhesion from a structurally dynamic shape-memory polymer. *ACS Appl. Mater. Interfaces* **2016**, *8*, 11041.
(93) Liu, J.; Scherman, O. A. Cucurbit[n]uril Supramolecular Hydrogel Networks as Tough and Healable Adhesives. *Adv. Funct. Mater.* **2018**, *28*, 1800848.
(94) Harada, A.; Kobayashi, R.; Takashima, Y.; Hashidzume, A.; Yamaguchi, H. Macroscopic self-assembly through molecular recognition. *Nat. Chem.* **2011**, *3*, 34.
(95) Liu, J.; Tan, C. S. Y.; Yu, Z.; Li, N.; Abell, C.; Scherman, O. A. Tough Supramolecular Polymer Networks with Extreme Stretchability and Fast Room-Temperature Self-Healing. *Adv. Mater.* **2017**, *29*, 1605325.

https://dx.doi.org/10.1021/jacs.9b12645
J. Am. Chem. Soc. XXXX, XXX, XXX−XXX